Characterization and Electrical Conductivity of Poly(ethylene glycol)/Polyacrylonitrile/Multiwalled Carbon Nanotube Composites

ARTICLE *in* JOURNAL OF APPLIED POLYMER SCIENCE · JANUARY 2011

Impact Factor: 1.77 · DOI: 10.1002/app.32326

2 AUTHORS:

Salem Aqeel
Oakland University, Rochester, MI, USA
14 PUBLICATIONS **32** CITATIONS
SEE PROFILE

Zuhal Küçükyavuz
Middle East Technical University
42 PUBLICATIONS **411** CITATIONS
SEE PROFILE

Characterization and Electrical Conductivity of Poly(ethylene glycol)/Polyacrylonitrile/Multiwalled Carbon Nanotube Composites

Salem M. Aqeel,[1] Zuhal Küçükyavuz[2]

[1]*Department of Chemistry, Faculty of Applied Science, Thamar University, P. O. Box 87246, Thamar, Yemen*
[2]*Department of Chemistry, Middle East Technical University, 06531 Ankara, Turkey*

Received 26 June 2009; accepted 15 February 2010
DOI 10.1002/app.32326
Published online 21 July 2010 in Wiley Online Library (wileyonlinelibrary.com).

ABSTRACT: Polymer blends based on poly(ethylene glycol), polyacrylonitrile, and multiwalled carbon nanotubes (MWNTs) were prepared by the solvent cast technique from the dispersion of the MWNTs in the concentration range 0–3.45 wt %. The interaction of the MWNTs with the polymer blend was confirmed by a Fourier transform infrared (FTIR) spectroscopy study. The thermal properties of the polymer blend with the MWNTs were carried out by means of differential scanning calorimetry (DSC). It was evident from DSC that the polymer/MWNTs had a high thermal stability. Scanning electron microscopy was used to study the dispersion of the MWNTs in the polymer blend. To measure the electrical conductivity, the four-point probe method was used. The electrical conductivity showed an ionic conductivity on the order of 4.4×10^{-4} to 1.2×10^{-2} S/cm. Relative changes in the conductivity with the concentration and temperatures for the samples were analyzed. © 2010 Wiley Periodicals, Inc. J Appl Polym Sci 119: 142–147, 2011

Key words: blends; differential scanning calorimetry (DSC); electron microscopy; FTIR; nanocomposites

INTRODUCTION

As nanoscience and nanotechnology have advanced rapidly, extensive research and development have been performed on high-performance polymeric nanomaterials for targeted applications in numerous industrial fields. Several attempts have been made to develop high-performance polymer nanocomposites with the benefit of nanotechnology in fields ranging from the scientific to the industrial, including the incorporation of nanoscaled reinforcements into the polymer matrix. Carbon nanotubes (CNTs) have attracted a great deal of interest as advanced reinforcements since CNTs were discovered by Iijima in 1991.[1] Moreover, this discovery has created a high level of activity in materials research, which has led to the practical realization of the extraordinary properties of CNTs, with their infinite number of possibilities for new materials.[2–5]

The incorporation of nanoparticles into a polymer matrix has been of increasing interest in materials engineering.[6–9] The resulting products are composite materials where nanoparticles are randomly dispersed. In this regard, polymers are a good choice as host materials because they have a wide variety of bulk physical properties and possess flexible processability.[10] Several works have appeared in the literature in which the preparation of new nanoparticles/polymer composites have been reported.[11–15] Commonly, a problem persists for these types of materials; particles of different types develop self-aggregation, and as a result, an uncontrollably wide size distribution occurs. Consequently, the development of easier synthesis techniques to produce new nanoparticles and nanodispersions with narrower size distributions in a polymer matrix is an actual challenge.

CNTs have exhibited remarkable chemical, electronic, and mechanical properties.[16,17] The tensile modulus and strength of CNTs reach 270 GPa-1 TPa and 11–200 GPa, respectively.[18] Polymer composites with CNTs are expected to improve the mechanical properties of matrix polymers. Lee et al.[19] prepared multiwalled carbon nanotube (MWNT)-reinforced polyurethane nanocomposites with excellent mechanical properties, thermal properties, and electric conductivity; their study showed that hydrogen bonding played an important role in the mechanical properties and that MWNTs had a strong influence on hard-segment hydrogen bonding. Kim et al.[20] studied the electrical conductivity of a film-typed sample of the MWNT/polystyrene (PS) composites

Correspondence to: S. M. Aqeel (salemaqeel@yahoo.com).
Contract grant sponsor: Erasmus Mundus External Cooperation Window Project for Post-doctoral Research European Union (EU).

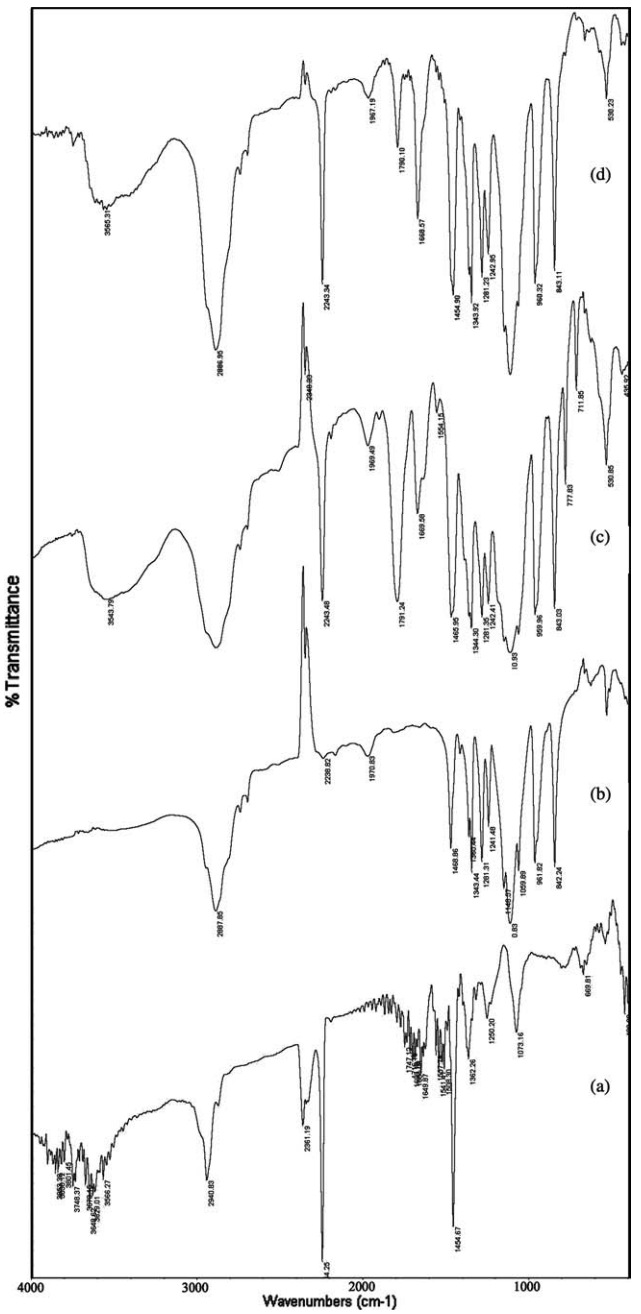

Figure 1 FTIR spectra of (a) PAN, (b) PEG, and the (c) PEG/PAN and (d) PEG/PAN/MWNT composites.

as a function of the MWNT content in PS; it was shown that the electrical conductivity with MWNT content in the PS was in accordance with a percolation theory,[21] and the percolation threshold for the MWNT/PS composites was between 0.5 and 1.0 wt %.

Miscible polymer blends are attractive host materials to which CNTs can be inserted because this type of mixture has a degree of mixing down to the molecular level. Many literature reports deal with the addition of CNTs as fillers into polymer matrices; however, just a few researchers have investigated the effect of adding CNTs to a polymer matrix specifically formed by a miscible polymer blend. Because CNTs are typically insoluble in organic solvents and severely bundled, their homogeneous dispersion in a desired polymer matrix is difficult to

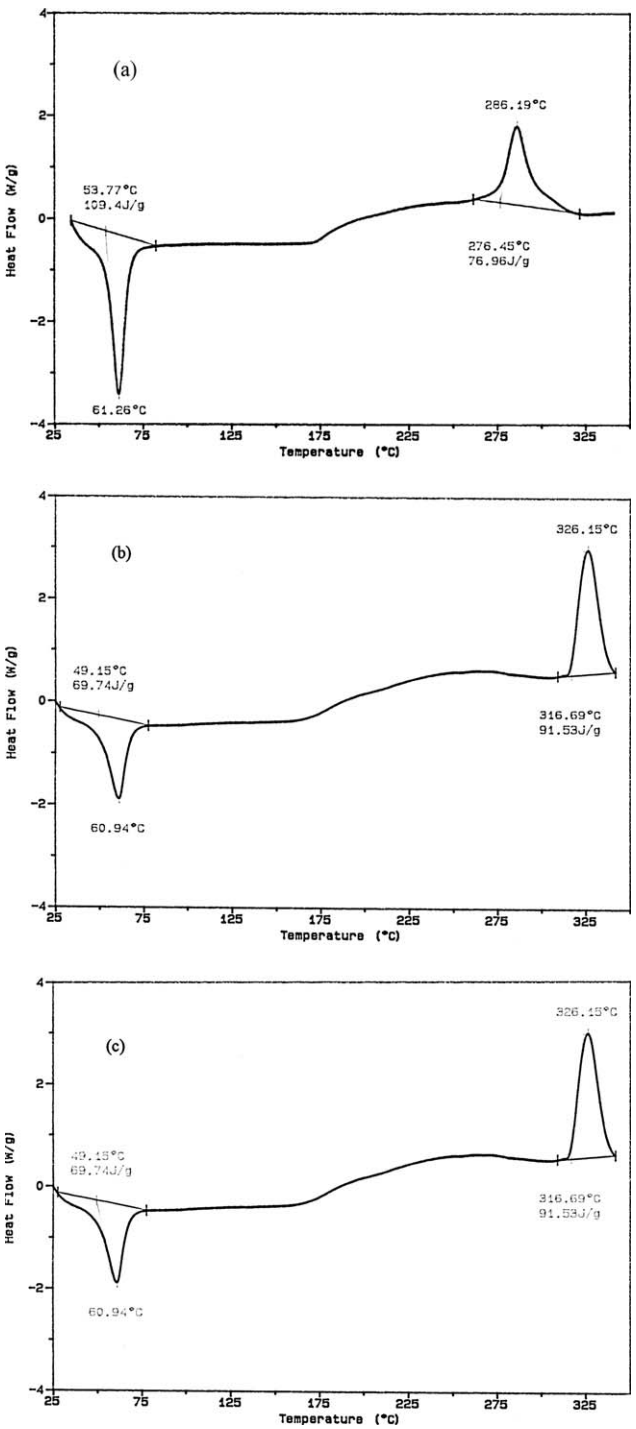

Figure 2 DSC heating curves for the (a) PEG/PAN blend and PEG/PAN/MWNT composites containing (b) 1.25 and (c) 3.45 wt % MWNTs.

TABLE I
Thermal Properties of the PEG/PAN/MWNT Composites

Sample	ΔH_m (J/g)	T_m (°C)	ΔH_c (J/g)	T_c (°C)	T_g (°C)
PEG			154.40	59.81	26.2
PAN	343.6	295.18			
PEG–PAN (30 : 70 wt %)	318.8	285			
PEG–PAN (50 : 50 wt %)	76.96	286.19	109.4	61.26	38
PEG–PAN (70 : 30 wt %)		287.16	89.02	59.14	36
PEG–PAN–MWNT (1.25 wt % MWNT)	20.59	292.70	47.79	58.25	
PEG–PAN–MWNT (2.36 wt % MWNT)	56.6	310	41	59.2	
PEG–PAN–MWNT (3.45 wt % MWNT)	91.53	326.15	69.47	60.94	

ΔH_m = heat of melting, ΔH_c = heat of crystallization, T_g = glass transition temperature.

achieve. The dissolution of CNTs in common organic solvents has been described.[22–25]

The aim of this study was to report on the thermal properties of polymer/MWNT composites. Differential scanning calorimetry (DSC) and Fourier transform infrared (FTIR) spectroscopy techniques allowed us to detect changes in the thermal and structural properties of the composites prepared as a function of the MWNT content. In addition, the morphology and electrical properties of the polymer composites were also examined.

EXPERIMENTAL

Poly(ethylene glycol) (PEG) with an average molecular weight of 2700–3300 was obtained from Merck (Darmstadt, Germany), polyacrylonitrile (PAN) with a molecular weight of 9.5×10^4 and dimethylformamide (DMF) were obtained from Aldrich Chemical Co. Inc. (Milwaukee, Wisconsin), and MWNTs with a diameter of 10 nm, a length of 0.1–10 μm, and a purity of 90% were supplied by Nanocyl S. A. (Hamburg, Germany). The blends were prepared by solution casting with DMF as a solvent. In the first part of the study, PEG and PAN were blended at several weight percentage ratios and dissolved in DMF. The solutions were stirred overnight and then poured into glass dishes and allowed to evaporate slowly at room temperature. The solid films were further dried *in vacuo* to remove residual solvent. The selected weight ratio of PEG to PAN (50 : 50) was selected for the second part of the experiments. Here, different weights of MWNTs (0.68, 1.25, 2.36, and 3.45 wt %) were mixed into PEG/PAN at the chosen ratio. The characterization of the samples was carried on a Nicolet DX 510 FTIR spectrometer with KBr pellets (analytical reagent grade) at room temperature. DSC measurements were carried out on a DuPont 2000 DSC instrument in standard mode with nitrogen gas. Samples were heated to 350°C with a heating rate of 10°C/min. The morphology of the composite was observed with scanning electron microscopy (SEM; model JSM-6400, JEOL, Peabody, MA, low voltage = 20 kV). The SEM samples were gold-sputtered to prevent charging. The electrical conductivity of the samples was measured at different temperatures with a four-probe technique (EPP 0602, Entek Electronics).

RESULTS AND DISCUSSION

The FTIR spectra of the PEG/PAN/MWNT composites were analyzed to confirm the interaction between the polymer blends and the MWNTs. The PEG/PAN/MWNT spectrum showed absorbance peaks at 1454 cm^{-1} (—CH_3), 2243 cm^{-1} (CN), 2886 cm^{-1} (—CH_2—), and 3565 cm^{-1} (O—H), characteristic of the polymer composite. The inset in Figure 1 demonstrates a small shift of the C≡N and OH peaks following the MWNT embedding compared with the pure PAN and PEG/PAN blend. The C≡N band, originally appearing at 2214 cm^{-1}, shifted slightly to 2243 cm^{-1} for the PEG/PAN/MWNT composite; however, it was evident that the OH peak for PAN/PEG/MWNT (3565 cm^{-1}) shifted compared to the PEG/PAN blend (3543 cm^{-1}).

DSC thermograms provide high information tools for studying the phase behavior of polymer blends and composites.[26] Figure 2 shows typical DSC curves of the PEG/PAN and PEG/PAN/MWNTs systems in the range 25–350°C; a single, sharp crystallization peak was observed for all of the blend compositions.

The linear relationship between the crystallization temperature (T_c) or melting temperature (T_m) and the blend composition indicated the additive contribution of the polymer blend to the total crystallinity; the DSC data are summarized in Table I. PEG showed an endothermic peak at 59.81°C (peak temperature), with a crystallization enthalpy of 154.40 J/g and a weak inflection or exothermic change in its base line at 121°C. This effect, demonstrated by other authors for PEG with different molecular weights,[27] was related to the oxidation of the PEG at this temperature. PAN exhibited a sharp exothermic peak between about 285 and 300°C. This peak corresponded to the dehydrogenation, oxidation, crosslinking, and mainly, cyclization reactions.

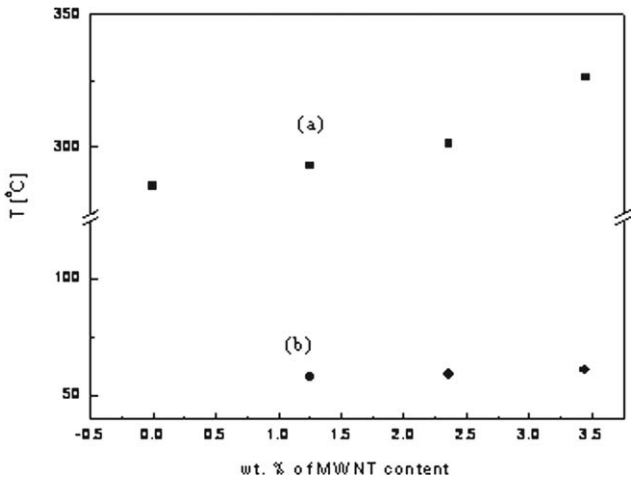

Figure 3 (a) T_m and (b) T_c of the PEG/PAN/MWNT composites as a function of the MWNT content.

The appearance of multiple melting peaks in some samples can usually be explained by the coexistence of different crystal populations or alternatively by melting and crystallization. The single glass transition meant that the polymer blend took a homogeneous single phase at the annealing temperatures. Figure 3 represents the effect of the MWNT composition on the T_m and T_c values of the PEG/PAN/MWNTs; there was an apparent increase in the T_m of the PEG/PAN film from 286.19°C to approximately 326°C in the blend with increasing MWNT content (0–3.45 wt %). Similar observations were made by Nam et al.[28] They reported that the T_m values of a poly(vinylidene fluoride) (PVDF) blended with MWNTs at various contents (0.01–5 wt %) increased from 177.9 to 182.1°C.

The T_c difference between the PEG/PAN blend and the samples containing MWNTs was very small; this indicated that the addition of the MWNTs did not significantly affect the value of T_c. That could have been due to the fact that the addition of CNTs to the blend inhibited crystallization.

Figure 4(a) shows the SEM micrograph of the MWNTs used in this study. The existence of a highly entangled networklike structure of the MWNTs is well evident in the micrograph. A percolated MWNT network structure and a relatively good dispersion of MWNTs were evident in the PEG/PAN/MWNT composites with 3.45 wt % MWNTs at different scales [Fig. 4(b,c)]. Compared to polymer/MWNTs prepared via an *in situ* bulk polymerization, the solvent cast film showed a better nanoscopic dispersion of MWNTs.[29]

The measurements of the ionic conductivity of the PEG/PAN/MWNT composites were carried out at different concentrations in the temperature range 293–353 K. The conductivity (σ)-temperature variations of the polymer composite were calculated as follows:[30]

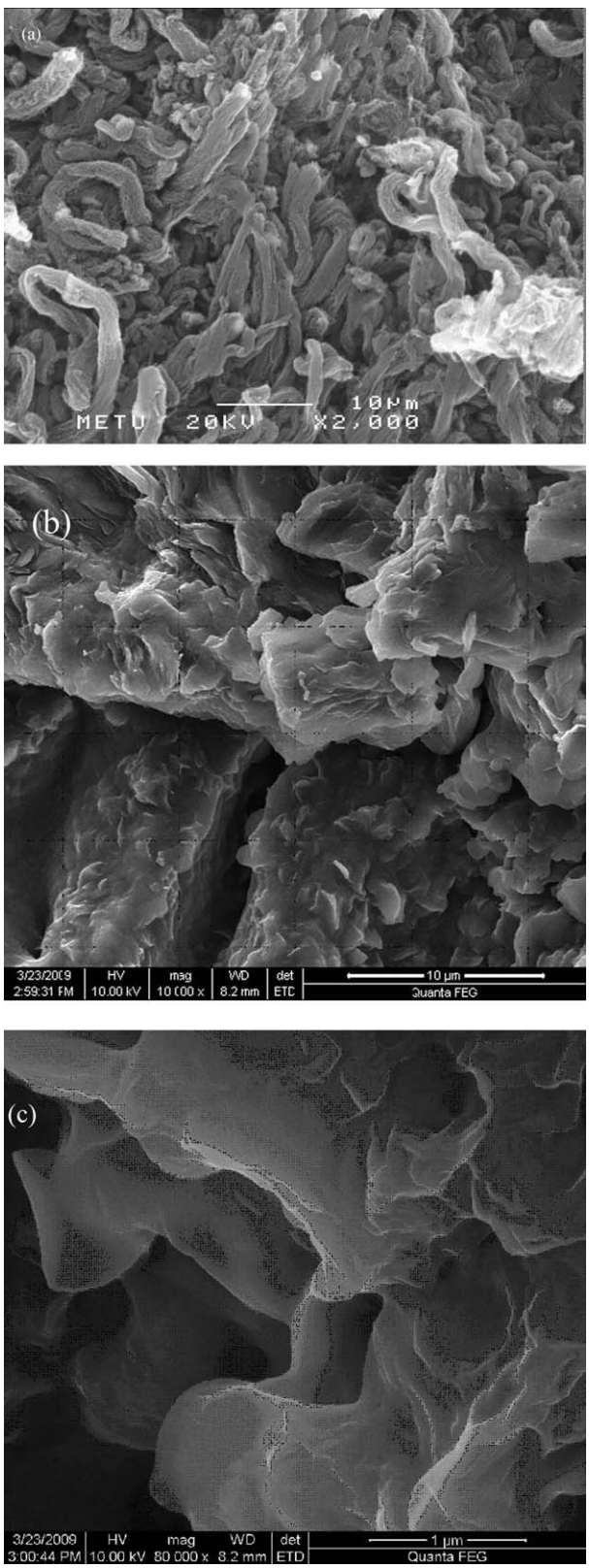

Figure 4 SEM micrographs for the (a) pure MWNTs and (b,c) PEG/PAN/MWNT in different scales.

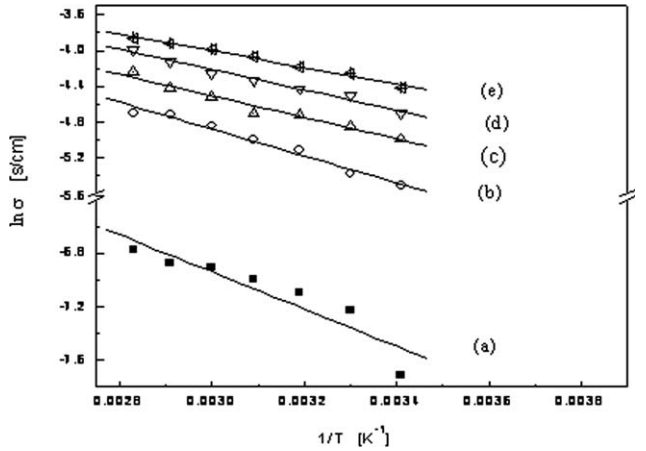

Figure 5 Arrhenius plots of the PEG/PAN/MWNT composites with (a) 0, (b) 0.68, (c) 1.25, (d) 2.36, and (e) 3.45 wt % MWNTs.

$$\sigma = \sigma_o \exp\left[\frac{-E_a}{kT}\right] \quad (1)$$

where E_a is the conductivity activation energy, K is Boltzmann's constant, and σ_o is the pre-exponential factor and includes the charge carrier mobility and density of state. The semilogarithmic plots of ln σ versus T^{-1} (temperature), illustrated in Figure 5, were linear with E_a values of 119 and 81 meV for PEG/PAN and PEG/PAN/MWNTs, respectively. The corresponding values of E_a are shown in Table II.

The electrical conductivity of PEG/PAN (50 : 50 wt %) was 4.4×10^{-4} S/cm; this result was comparable with the polymer blend by Liang et al.[31] With the variation of PAN, although the conductivity changed, the values were in the range of 10^{-3} orders of magnitude. However, a change in the amount of PAN had a considerable effect on the mechanical properties. These observations led to the conclusion that PAN played a great role in providing mechanical stability rather than conductivity.[32]

The highest electrical conductivity was given by the sample containing 3.45 wt % MWNTs with a conductivity of 1.2×10^{-2} S/cm. Figure 6 presents the conductivity of the PEG/PAN/MWNT composites as a function of the MWNT composition. The analysis was carried out at room temperature. This

TABLE II
Arrhenius and Vogel-Tamman-Fulcher (VTF) Activation Parameters for the PEG/PAN/MWNTs

MWNTs (wt %)	σ_o	E_a (meV)
0	0.06204	119
0.68	0.69643	130
1.25	0.4182	104
2.36	0.44844	97.9
3.45	0.30821	81.1

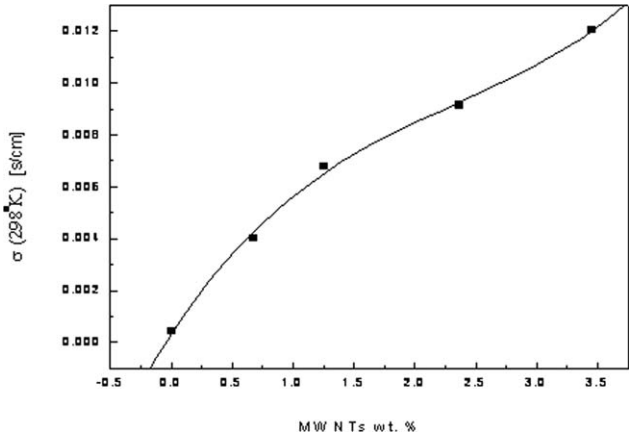

Figure 6 Electrical conductivity of the PEG/PAN/MWNT composites as a function of the MWNT content.

graph clearly shows that conductivity increased to the maximum value at 3.45 wt % MWNTs. The percolation threshold for the PEG/PAN/MWNTs was around 0.625 wt % MWNTs. However, Hu et al.[33] reported that the tunneling effect could be identified by the increase in the electrical conductivity when the volume fractions of CNTs were near the percolation threshold of the composite. The tunneling effect disappeared gradually with increasing addition of CNTs. This result implies that a high sensitivity in strain measurement could be achieved in this nanocomposite when the CNT loading was controlled to be close to the percolation threshold.

The conductivity of the PEG/PAN blend at room temperature was reported to be 4.4×10^{-4} S/cm. Similar observations were obtained by Sundaray et al.[34]; it was indicated that the conductivity of the PMMA/MWNTs further increased by nearly one order of magnitude from 4.5×10^{-5} to 5.3×10^{-4} S/cm with increasing concentration of the MWNTs from 0.05 to 2 wt %. This was possibly due to its high conductivity.

CONCLUSIONS

The studied PEG/PAN/MWNT composites were prepared by a solvent cast technique. The microstructure, thermal properties, and electrical conductivity of four MWNT-filled polymer blend systems were investigated and analyzed. We concluded that the MWNT distribution in the polymer blend played a very important role in the determination of both the thermal and electrical properties of all of the composites. It was evident that the polymer/MWNTs had a high thermal stability. The electrical conductivity showed an ionic conductivity on the order of 4.4×10^{-4} to 1.2×10^{-2} S/cm. The percolation threshold for the PEG/PAN/MWNTs was around 0.625 wt % MWNTs. Nanocomposites based

on PEG/PAN and MWNTs as filler showed a significant enhancement in the electrical conductivity as a function of temperature. The good electrical properties of the composites containing MWNTs are promising for the design of low-cost polymer composites for numerous future applications.

References

1. Iijima, S. Nature 1991, 354, 56.
2. Iijima, S.; Ichihashi, T. Nature 1993, 363, 603.
3. Wong, E. W.; Sheehan, P. E.; Lieber, C. M. Science 1997, 277, 1971.
4. Pirlot, C.; Willems, I.; Fonseca, A.; Nagy, J. B.; Delhalle, J. Adv Eng Mater 2002, 4, 109.
5. Yu, M. F.; Lourie, O.; Dyer, M. J.; Moloni, K.; Kelly, T. F.; Ruoff, R. S. Science 2000, 287, 637.
6. Berber, S.; Kwon, Y. K.; Tomanek, D. Phys Rev Lett 2000, 8420, 4613.
7. Sluzarenko, N.; Heurtefeu, B.; Maugey, M.; Zakri, C.; Poulin, P.; Lecommandoux, S. Carbon 2006, 44, 3207.
8. Tian, Y.; He, Q.; Cui, Y.; Tao, C.; Li, J. Chem—Eur J 2006, 12, 4808.
9. Deng, J.; Cao, J.; Li, J.; Tan, H.; Zhang, Q.; Fu, Q. J Appl Polym Sci 2008, 108, 2023.
10. Guo, H.; Sreekumar, T. V.; Liu, T.; Minus, M.; Kumar, S. Polymer 2005, 46, 3001.
11. Lin, S.; Wei, K.; Lee, T.; Chiou, K.; Lin, J. Nanotechnology 2006, 17, 3197.
12. Bose, S.; Bhattacharyya, A. R.; Kodgire, P. V.; Misra, A.; Potschke, P. J Appl Polym Sci 2007, 106, 3394.
13. Han, S. J.; Kim, B.; Suh, K. D. Macromol Chem Phys 2007, 208, 377.
14. Wu, M.; Shaw, L. J Appl Polym Sci 2006, 99, 477.
15. Corbierre, M. K.; Cameron, N. S.; Sutton, M.; Mochrie, S. G. J.; Lurio, L. B.; Ruhm, A.; Lennox, R. B. J Am Chem Soc 2001, 123, 10411.
16. Shafer, M. P.; Windle, A. H. Adv Mater 1999, 111, 937.
17. Inagaki, M.; Kaneko, K.; Nishizawa, T. Carbon 2004, 42, 1401.
18. Lau, K. T.; Hui, D. Compos B 2002, 33, 263.
19. Lee, C.; Liu, J.; Chen, S.; Wang, Y. Polym J 2007, 39, 138.
20. Kim, S. T.; Choi, H. J.; Hong, S. M. Colloid Polym Sci 2007, 285, 593.
21. Stauffer, D. Introduction to Percolation Theory; Taylor & Francis: London, 1985.
22. Breuer, O.; Sundararaj, U. Polym Compos 2004, 25, 630.
23. Xia, H.; Song, M.; Jin, J.; Chen, L. Macromol Chem Phys 2006, 207, 1945.
24. Antolın-Ceron, V. H.; Gomez-Salazar, S.; Soto, V.; Avalos-Borja, M.; Nuno-Donlucas, S. M. J Appl Polym Sci 2008, 108, 1462.
25. Sun, Y.; Wilson, S. R.; Schuster, D. I. J Am Chem Soc 2001, 123, 5348.
26. Feldstein, M. M.; Shandryuk, G. A.; Kuptsov, S. A.; Plate, N. A. Polymer 2000, 41, 5327.
27. Arias, M. J.; Moyano, J. R.; Gines, J. M. Thermochim Acta 1998, 321, 33.
28. Nam, Y. W.; Kim, W. N.; Cho, Y. H.; Chae, D. W.; Kim, W. H.; Hong, S. P.; Hwang, S. S.; Hong, S. M. Macromol Symp 2007, 249, 478.
29. Park, S. J.; Cho, M. S.; Lim, S. T, Choi, H. J.; Jhon, M. S. Macromol Rapid Commun 2005, 26, 1563.
30. Paul, D. K.; Mitra, S. S. Phys Rev Lett 1973, 31, 1000.
31. Liang, Y. H.; Wang, C.; Chena, C. J Power Sources 2007, 172, 886.
32. Perera, K. S.; Dissanayake, M. A.; Skaarup, S.; West, K. J Solid State Electrochem 2008, 12, 873.
33. Hu, N.; Karube, Y.; Yan, C.; Masuda, Z.; Fukunaga, H. Acta Mater 2008, 56, 2929.
34. Sundaray, B.; Subramanian, V.; Natarajan, T. S.; Krishnamurthy, K. Appl Phys Lett 2006, 88, 143114.